

Axion Searches with Helioscopes and astrophysical signatures for axion(-like) particles

K Zioutas^{1,2}, M Tsagri^{1‡}, Y Semertzidis³, T Papaevangelou⁴,
T Dafni⁵ and V Anastassopoulos¹

¹ University of Patras, Patras, Greece

² European Organization for Nuclear Research (CERN), CH-1211 Genève 23, Switzerland

³ Brookhaven National Laboratory, NY-USA

⁴ IRFU, Centre d' Études Nucleaires de Saclay, Gif-sur-Yvette, France

⁵ Laboratorio de Física Nuclear y Astropartículas, Universidad de Zaragoza, Zaragoza, Spain

E-mail: Thomas.Papaevangelou@cern.ch

Abstract. Axions should be produced copiously in Stars such as the Sun. The first part of the article reviews the capabilities and performance of axion helioscopes. The mechanism they rely on is described and the achieved experimental results for the interaction of solar axions and axion-like particles with matter are given. The second part is actually observationally driven. New results obtained with Monte Carlo simulation reconstruct solar observations, previously dismissed, supporting an axion(-like) involvement with $m_a \approx 1-2 \times 10^{-2} \text{ eV}/c^2$. To further quantify the suggested solar observations as being originated by axions, additional theoretical work is needed. However, the recently suggested axion interaction with magnetic field gradients is a generic theoretical example that seems to reconcile for the first time present limits, derived from axion helioscopes, and potential axion-related solar X-ray activity, avoiding thus contradictions with the best experimental limits. Magnetic quadrupoles can be used to experimentally test this idea, thus becoming a new catalyst in axion experiments. Finally, a short outlook for the future is given, in view of the experimental expansion of axion research with the state-of-the-art orbiting X-ray observatories.

‡ Present address: European Organization for Nuclear Research (CERN), CH-1211 Genève 23, Switzerland

1. Motivation

The recent WMAP measurements [1] have established with great precision that, about 84% of the matter content of the Universe is in the form of cold dark matter (CDM). The composition of CDM is not yet known, however the most promising particle constituents are WIMPs (Weakly Interacting Massive Particles) and axions. In this work, we focus on the axions. The theoretically introduced axions have far reaching consequences in astrophysics and cosmology. At the theoretical level, the imprint of axions appears in the QCD Lagrangian, which includes a CP-violating parameter, the θ -QCD ($\bar{\theta}$):

$$L_{CPV} = \bar{\theta} \frac{\alpha_s}{8\pi} G\tilde{G}, \quad (1)$$

where a_s is the strong coupling constant and G and \tilde{G} represent the gluon field and its dual. From this one can estimate within an order of magnitude the neutron EDM [2, 3]:

$$d_n(\bar{\theta}) \approx \bar{\theta} \frac{e}{m_n} \frac{m_*}{\Lambda_{QCD}} \approx \bar{\theta} \cdot (5 \times 10^{-17}) e \cdot \text{cm}, \quad (2)$$

with $m_* = (m_u m_d)/(m_u + m_d)$ being the reduced mass of the up and down quarks. Λ_{QCD} is the QCD scale (~ 200 MeV) and m_n the neutron mass. When the estimation is done more precisely [4–7] it comes out as $d_n(\bar{\theta}) \approx \bar{\theta} \cdot (3.6 \times 10^{-16}) e \cdot \text{cm}$. The present neutron EDM limit [8] of $3 \times 10^{-26} e \cdot \text{cm}$ results to a limit on θ -QCD of $\bar{\theta} \leq 10^{-10}$. With the planned dEDM and pEDM experiments at BNL, the experimental sensitivity can reach the level of $\bar{\theta} \leq 10^{-13}$.

The value of $\bar{\theta}$ could potentially be between 0 and 2π . However, it turns out to be extremely tiny, apparently due to some fine tuning mechanism. There is no symmetry reason within the Standard Model for such a small value, creating the so-called strong CP problem. Peccei and Quinn postulated that such a tiny value arises from the breakdown of a new symmetry, which gives rise to axions [9–13]. The latter are pseudoscalar particles arising as a solution to the CP problem in strong interactions. They have properties closely related to those of neutral pions. That is to say, the discovery of a QCD inspired axion will explain why $\bar{\theta}$ is extremely small. Apart from all this, axions also appear in string theory.

The standard axions were thought to have a symmetry-breaking scale (or axion decay constant) of the order of the electroweak scale [12, 13]. However, after such scenarios were ruled out, new models were developed where that scale was arbitrary. In fact, it could be so large that would make axions interact so weakly that they were dubbed ‘invisible’. Such were the first, thoroughly cited, axion models following the work of Kim-Shifman-Vainshtein-Zakharov (KSVZ) [14, 15] and Dine-Fischler-Srednicki-Zhitnitskii (DFSZ) [16, 17].

In order to detect axions, one could rely on the generic property of axions to couple to two photons [18], as described by the Lagrangian term

$$\mathcal{L}_{a\gamma\gamma} = -\frac{1}{4} g_{a\gamma\gamma} F_{\mu\nu} \tilde{F}^{\mu\nu} a = g_{a\gamma\gamma} \mathbf{E} \cdot \mathbf{B} a, \quad (3)$$

where a is the axion field, F is the electromagnetic field-strength tensor, \tilde{F} its dual, \mathbf{E} and \mathbf{B} the electric and magnetic field, respectively.

Over the last three decades, different experimental techniques have been developed for the search of the ‘invisible axions’ or, more generally, ‘axion-like particles’: cavity searches for galactic matter axions [18–23], solar axion searches using ‘helioscopes’ [18, 23–31], the Bragg scattering technique [32–35], the polarization of light propagating through a transverse magnetic field [36–39], photon regeneration [38, 40–49] and others like the resonant method involving nuclear couplings [50–54]§.

The second part of the article is observationally driven. We suggest atypical solar axion signatures as the so far unnoticed manifestation of axions or axion-like particles (ALPs), which fit decades-old puzzling solar observations and every day’s experience of solar X-ray telescopes. To better understand relevant observations from the ubiquitously magnetized solar surface within the axion or axion-like scenario, Monte Carlo simulations have been performed, revising for the first time the propagation of magnetically converted axions [55] near the solar surface, that is, the created X-rays. This is due to isotropic Compton scattering of X-rays coming from axion conversion underneath the lower chromosphere or even higher in the dynamic atmosphere. For the conversion to happen efficiently, e.g. to ensure a large axion-to-photon coherence length, it is reasonable to assume that the axion rest mass must match the local plasma density ($m_a c^2 \approx \hbar \omega_{pl}$). To reconcile magnetic field-related solar X-ray observations and the axion scenario, the derived rest mass is, within a factor of 2-3, $m_a \approx 10 \text{ meV}/c^2$, which coincides with the upper limit derived from SN1987A [56], while cosmological data allow for an axion rest mass below $\sim 1 \text{ eV}/c^2$ [57].

In fact, star evolution arguments exclude the involvement of axions or the like (up to a certain coupling strength) [56, 58]. In this work, we look more specifically at solar X-ray observations as potential signatures for new exotica, with preference to faint intensities, whose luminosity cannot actually affect stellar evolution. With this, however, we do not exclude a priori large flaring events as being powered -or at least triggered- by solar exotica.

Other, recently published work [59–64], refers to signatures on very light ALPs (assuming $m_a \ll 10^{-7} \text{ eV}/c^2$) via the oscillatory behaviour of cosmic very high energy (VHE) light and ALPs as they propagate over billions of years through the intergalactic magnetic network. While the QCD-inspired axion implies a particle with one rest mass and one coupling constant, ALPs do not have to follow this constrain. As an example, we mention the massive axions of the Kaluza-Klein type [65], which have a tower of mass states, but one common coupling constant.

Throughout this work, references to the solar axion scenario include any other particle candidate with similar properties (ALPs).

§ A simple comparison between the methods, showing that the magnetic helioscopes are more effective than the (crystalline) detectors, can be done by calculating that $(0.1 \text{ T m})^2$ corresponds to a detector thickness of $2Z^{-1} \text{ kg}/\text{cm}^2$, where Z the atomic number of the detector material.

2. Solar axion flux

The Lagrangian term (3) points to the $\mathbf{E} \cdot \mathbf{B}$ in a hot thermal plasma as a source for the production of axions. \mathbf{E} is provided by the charged particles of the plasma whereas \mathbf{B} arises from propagating thermal photons. The Primakoff process describes an incoherent production, where a photon converts into an axion in the electric field of a charged particle (Figure 1). Figure 2 shows the axion flux spectrum as expected at the Earth; it is, essentially, a blackbody distribution of the thermal conditions in the solar interior, which presents a maximum at the energy of 3 keV and a mean energy value of $\langle E \rangle = 4.2$ keV. The reason for the higher energy than the one in the Sun hot core ($kT \sim 1$ keV) is the suppression of low energies (large wavelengths) which reaches in total a factor of ~ 25 due to screening effects [67]. An analytic approximation of the

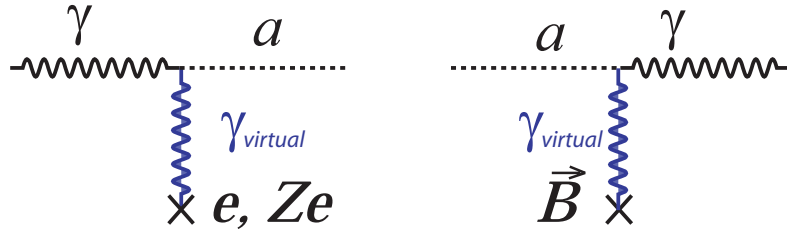


Figure 1. Left: The incoherent Primakoff effect, which is assumed to occur inside the hot solar core and which gives rise to the creation of axions. Right: The inverse coherent process in a magnetic field, which is so far the working principle of an axion helioscope as it transforms the otherwise ‘invisible’ axions to observable photons. This is an oscillation phenomenon, analogous to neutrino oscillations. The external magnetic field is needed in order to compensate the spin-mismatch in the case of photon-axion oscillation [61].

flux is given by [30]:

$$\frac{d\Phi_a}{dE} = 6 \times 10^{10} \text{ cm}^{-2} \text{ s}^{-1} \text{ keV}^{-1} g_{10}^2 E^{2.481} e^{-E/1.205} \quad (4)$$

where Φ_a is the axion flux and $g_{10} = g_{a\gamma\gamma}/10^{-10} \text{ GeV}^{-1}$. This equation takes into account the Primakoff effect of real thermal photons interacting with the Coulomb electric field of the solar core plasma in atomic scale. Most of the axion flux emerges from $R \lesssim 0.1R_\odot$ or from $\sim 2\%$ of the solar disk surface (for an earth-bound observer).

So far, the impact of the solar magnetic fields has been widely ignored. This point will be addressed in (sections 6 and 7). Some fine tuning cannot be excluded, taking into account the variations of the dynamic Sun in all spatio-temporal scales, in particular in the outer layer ($R \gtrsim 0.9R_\odot$). The inner solar magnetic field must reach approximately

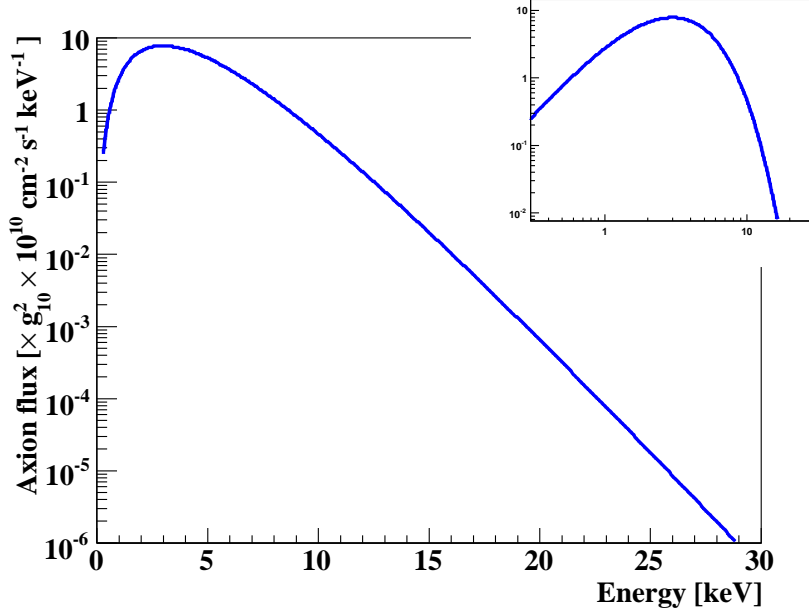


Figure 2. The solar axion flux as expected at the Earth, following relation 4, plotted in log-linear and log-log scales (inserted). The spectrum has a peak at around 3 keV and mean energy of 4.2 keV. The sub-keV range was experimentally not accessible before. Recently, first measurements have started covering the few-eV energy range [66]. Axion helioscopes are the best suited for low energy searches, since the screening effects, which appear in dense materials, are quasi-suppressed.

50 to 100 T at the bottom of the convection zone (about 200 000 km below the surface, i.e. at $R \simeq 0.7 R_{\odot}$), while even much higher fields might exist deeper in the Sun [68].

3. Principles of Detection

The search for solar axions with helioscopes is based on the inverse coherent Primakoff effect (Figure 1): solar axions coming from the Sun (produced via the incoherent Primakoff effect) will be re-converted to X-ray photons as they pass through a (strong) transverse laboratory magnetic field. These excess photons would then be seen in X-ray detectors [18], located outside the actual magnetic field region. The number of photons expected to reach these detectors is

$$N_{\gamma} = \int \frac{d\Phi_a}{dE} P_{a \rightarrow \gamma} A t dE \quad (5)$$

where $d\Phi_a/dE$ is the axion spectrum as expected at the Earth (4), $P_{a \rightarrow \gamma}$ the probability of the axion-to-photon conversion, t the observation time and A the axion-sensitive area of the magnet aperture. The conversion probability is expressed as

$$P_{a \rightarrow \gamma} = \left(\frac{g_{a\gamma} B}{2} \right)^2 \frac{1}{q^2 + \Gamma^2/4} [1 + e^{-\Gamma L} - 2e^{-\Gamma L/2} \cos qL] . \quad (6)$$

With Γ , the inverse absorption length in the medium, the general case of the presence of a refractive medium inside the magnetic pipes has been included. The axion-photon

momentum transfer q is given by $q = (m_a^2 - m_\gamma^2)/(2E_a)$ and m_γ is the effective mass of the photon as acquired due to the medium (see (15)). Substituting (6) and (4) in (5), we get

$$N_\gamma \simeq 10^{-6} \text{ cm}^{-2} \text{ s}^{-1} \text{ keV}^{-1} g_{10}^4 E^{2.481} e^{-E/1.205} \left(\frac{L}{10 \text{ m}} \right)^2 \left(\frac{B}{9.0 \text{ T}} \right)^2 A t dE. \quad (7)$$

This equation makes evident the importance of the factors B , L and A in the detection of axion-converted photons. To maintain the maximum conversion probability, i.e. zero momentum transfer ($q \rightarrow 0$), the axion and photon fields need to remain in phase over the length of the magnetic field. This coherence condition is met when $qL \lesssim \pi$, meaning that the experiment is sensitive to different mass ranges depending on q :

$$\sqrt{m_\gamma^2 - \frac{2\pi E_a}{L}} \lesssim m_a \lesssim \sqrt{m_\gamma^2 + \frac{2\pi E_a}{L}} \quad (8)$$

The fractional resolution can be written as:

$$\frac{dm_a}{m_a} \equiv \frac{dm_\gamma}{m_\gamma} = \frac{2\pi E_a}{L m_a^2}. \quad (9)$$

Taking an axion energy of $E_a=1 \text{ eV}$, $m_\gamma=10^{-3} \text{ eV}/c^2$ and $L=10 \text{ km}$, the width becomes

$$\frac{\text{FWHM}}{m} \simeq 1.2 \times 10^{-4}. \quad (10)$$

Further, for solar axions with $E_a=4.2 \text{ keV}$, $m=1 \text{ eV}/c^2$ and $L=4 \text{ m}$ [24],

$$\frac{\text{FWHM}}{m} \simeq 10^{-3} \left(\frac{m_\gamma}{\text{eV}} \right)^{-2}, \quad (11)$$

for $m_\gamma=0.1 \text{ eV}/c^2$, FWHM=10%.

When changing to fractional density, one obtains

$$\frac{d\rho}{\rho} = 2 \frac{dm}{m}. \quad (12)$$

Choosing $E_a=4.2 \text{ keV}$ and $m_a=10^{-2} \text{ eV}/c^2$, the allowed density fluctuations should not be more than $d\rho/\rho \simeq 10^{-2}$, in order to maintain the coherence effect over the whole length. For the static Sun these conditions are encountered at a few hundreds of km underneath the surface and the coherence length there can be $L \simeq 3 \text{ km}$ (to be compared, for example with the CAST 10 m length)||.

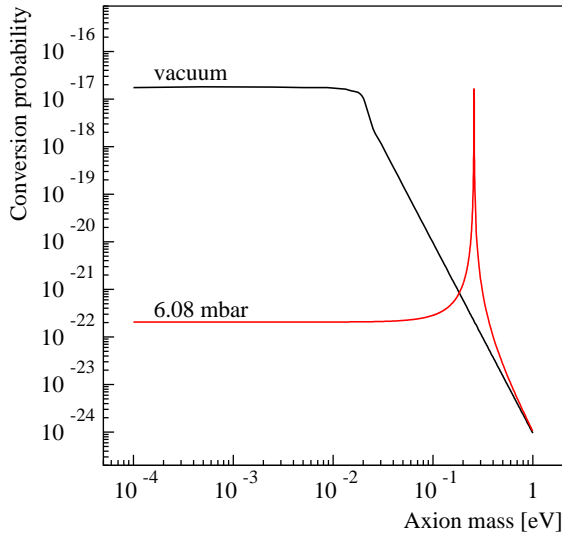


Figure 3. The axion-to-photon conversion probability versus the axion rest mass, assuming an axion-photon coupling constant of $g_{a\gamma\gamma}=1\times 10^{-10}\text{ GeV}^{-1}$. In black, the line corresponding to vacuum inside a 10 m long magnetic pipe at 9 T. For $m_a\geq 0.02\text{ eV}/c^2$, the conversion efficiency breaks down because the incident axion and the emerging photon waves get out of phase (deconstructive interference). In red, the conversion probability for a specific Helium density setting (equivalent to 6.08 mbar at 1.8 K). The shown resonance curve has a very narrow ($\sim 0.5\%$) width for which the specific pressure (density) of the refractive material (Helium gas) restores the coherence over the whole length [30].

3.1. Data-taking strategies

Vacuum In the particular case in which the magnetic field where axions are converted into photons is under vacuum ($\Gamma \rightarrow 0, m_\gamma \rightarrow 0$), equation (6) becomes [24]

$$P_{a\rightarrow\gamma} = \left(\frac{g_{a\gamma\gamma} B}{q} \right)^2 \sin^2 \left(\frac{qL}{2} \right), \quad (13)$$

while $q = m_a^2/2E_a$. Applying the coherence condition, the range of axion rest masses one is sensitive to is

$$m_a \lesssim \sqrt{\frac{2\pi E_a}{L}}. \quad (14)$$

This implies that for a magnetic field of $L=10\text{ m}$ and for a mean solar axion energy of 4.2 keV , the sensitivity of an experiment would cover axion rest masses of

|| Taking into account the Sun's dynamical character near its surface it is still reasonable to assume, as a numerical example, $L\approx 20\text{ km}$ and $B\approx 1\text{ T}$ [69]. This results to $P_{a\rightarrow\gamma}\approx 10^{-12}$ ($g_{a\gamma\gamma} = g_{10}$). For comparison, the surface X-ray brightness of a large flare requires instead a conversion efficiency of $\gtrsim 10^{-3}$. Then, the brightness of such events cannot be explained quantitatively only by QCD-axions using the inverse Primakoff effect, even assuming favourable input parameters. We do not reject these events from further consideration, since the rest of their behaviour fits the axion scenario of this work. Nevertheless, much lower X-ray brightenings, like microflares, nanoflares, etc., but also the quiet Sun itself, should then be more appropriate for the reasoning of this work (see section 6.2.4).

$m_a \lesssim 0.02 \text{ eV}/c^2$ (Figure 3).

Refractive gas More massive axions will begin to fall out of phase with the emerged photon waves, due to different velocities. The addition of a refractive material (a buffer gas, for example) will ‘slow’ the photon giving it an effective mass (m_γ). In order to compensate for the velocity mismatch and restore maximum conversion probability, m_γ should be adjusted to approach m_a . In a low- Z gas, where self absorption is minimum, the effective photon mass (m_γ) and the axion rest mass must fulfill the following condition [24]

$$m_a c^2 = m_\gamma c^2 = \hbar \omega_{pl} = \hbar \sqrt{\frac{4\pi\alpha n_e}{m_e}}, \quad (15)$$

in which α is the fine structure constant and m_e and n_e the electron mass and number density respectively ¶. For a rest mass of $1 \text{ eV}/c^2$, this would imply a required pressure at room temperature of almost 15 bar or, for the case of Helium in the cryogenic environment of a magnet (e.g. 1.8 K), a pressure of 90 mbar. Extending the calculations to the Sun surface, one finds $\hbar \omega_{pl} \simeq 10^{-2} \text{ eV}$ for $\rho = 2 \times 10^{-7} \text{ g}/\text{cm}^3$, or $\hbar \omega_{pl} \simeq 300 \text{ eV}$ in the core ($\rho=150 \text{ g}/\text{cm}^3$).

Different axion masses can be tuned by changing the gas density (pressure) in discrete steps. For each density, the coherence condition is restored, but only for a very narrow mass range around $m_\gamma = m_a$. For $m_a=1 \text{ eV}/c^2$, $L=10 \text{ m}$ and a mean axion energy of $E_a=4.2 \text{ keV}$, (9) and (12) imply a required constant density at a level of $d\rho/\rho \simeq 10^{-3}$. An example of the probability conversion for two different pressures (vacuum and 6.08 mbar) is given in Figure 3. To assure density homogeneity over the length of the magnetic pipes, even gravity effects have to be taken into account when tracking the sun with the magnet tilted. The effect of the gravity in the gas density in the magnetic cold bores along with the attenuation of the X-rays are the ultimate limits for the performance of an axion helioscope (for a detailed discussion, see [70]).

Another strategy of taking data with gas in the pipes is by performing a continuous ‘scanning’ over a large range of pressures during one solar tracking measurement. The advantage this approach provides with respect to the previous one is that it allows for a ‘fast-look’ to a wide range of axion rest masses, but with lower sensitivity. A possible signal candidate can be scanned later over longer time intervals, following a specific, predefined protocol procedure, excluding in this way any kind of bias in the selection. A similar ‘scanning’, but covering eventually a much wider density [=axion rest mass] range, is suggestive of taking place in the dynamic Sun (see section 6).

¶ Although in the actual experiments the refractive gases are not ionized, this equation holds as long as the axion/photon energies involved are much higher than the binding energy of the atomic electrons of the refractive gas. However, one needs to exercise cautiousness when applying this method searching for much lower energy solar axions, if their energy approaches that of atomic transitions.

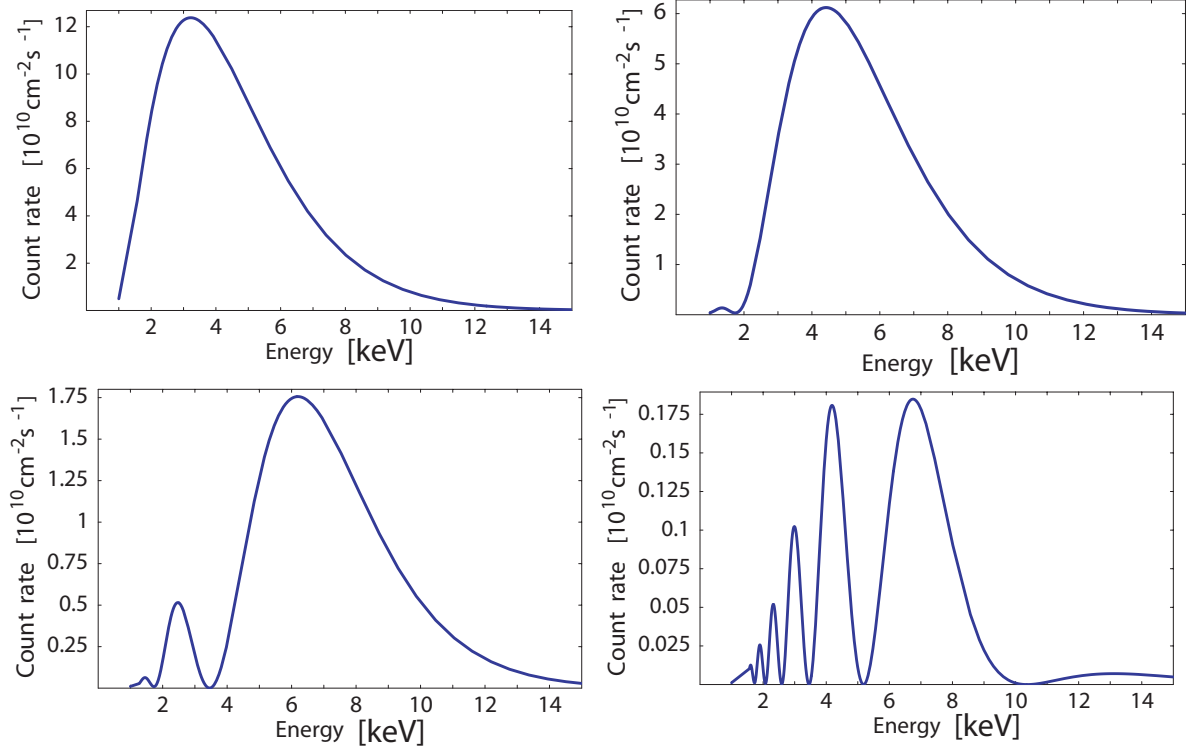


Figure 4. Expected analog photon spectra (assuming an axion-photon coupling constant $g_{a\gamma\gamma}=1\times 10^{-10}\text{ GeV}^{-1}$) depending on the shift $S=m_\gamma-m_a$ from the resonance: $S=0$ (top left), $S=0.5\times\text{FWHM}$ (top right), $S=\text{FWHM}$ (bottom left) $S=3\times\text{FWHM}$ (bottom right) [31]. Note the change of the spectral shape and decrease in intensity with increasing S .

4. Axion Identification Techniques

In this section we discuss three techniques that can be applied for the identification of an unambiguous solar axion signal, either individually or combined:

Excess Since axions are expected to oscillate into photons only while traversing a dipole magnetic field which is pointing at the centre of the Sun, one expects an excess in X-rays compared to the periods when the Sun is out of the field of view of the magnet (background). In the case of a signal candidate one has -in principle- the possibility to change the magnetic field, repeat the run and investigate whether the candidate signal follows the B^2 dependence dictated by (7). This is usually considered as the ultimate cross check, although increasing the field is hardly an option (given that one usually already runs at the maximum magnetic field, and running the magnet with significantly reduced field is not trivial either).

On/Off-resonance identification technique This technique allows to definitely and precisely establish a potential axion signal and its rest mass, provided that $m_a \gtrsim 0.01\text{ eV}/c^2$, for $L=10\text{ m}$. In addition, the CAST collaboration [31] for the first time explains how the spectral distribution of the axion-converted photons depends on the momentum mismatch between the axion and the emerging “massive” photon

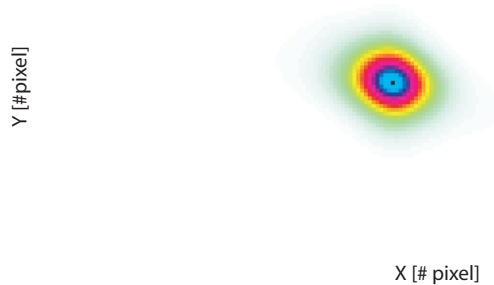


Figure 5. Simulation of the expected axion image of the Sun focusing the coherently converted axions-to-X-rays inside the magnetic field of CAST on the CCD pixel detector (64×200 pixels of $150 \mu\text{m} \times 150 \mu\text{m}$)[30].

m_γ (Figure 4). The striking oscillatory behaviour of the otherwise smooth solar axion spectrum provides an undoubtable signature.

Focusing devices The discovery potential of an axion helioscope is improved significantly by using an X-ray focusing device, as it has been implemented for the first time by the CAST collaboration. An X-ray telescope (or other focusing optics) presents a threefold importance: a) it projects all the axion-converted X-rays entering from the axion sensitive region (in general, the magnet aperture with a surface of tens of cm^2) onto a small spot of few mm^2 at the focal plane, thus increasing the S/B ratio by 1 or 2 orders of magnitude, b) it allows for a *simultaneous* measurement of signal (inside the spot area) and background (outside the expected spot), a unique possibility in general and c) as an imaging device, a strong signal resulting from axion-to-photon conversion will reflect the energy and radial intensity distribution of the inner Sun (Figure 5), with an unprecedented accuracy, having in mind for comparison the poor reconstruction with the solar neutrinos.

We point out that the working principles of both techniques, i.e. the excess as well as the on/off-resonance ID, apply to the Sun’s huge-sized magnetic fields. In fact, we use below both to understand otherwise unexplained and unpredictable spatio-temporally varying solar X-ray surface brightness.

5. Axion Helioscopes

In the following we describe the short list of the axion helioscopes built up to now.

5.1. The pioneering axion telescope

The first axion helioscope was built in 1992 by the Rochester-Brookhaven-Fermi collaboration [25], following the recipe given in [18]. Their ‘axion converter’ was a 2.2 T dipole magnetic field extended over 1.8 m. This magnet, lying fixed, was oriented towards the setting of the Sun in such a way that it would actually point directly to the Sun during ~ 15 min for a few days. For the detection of the converted axions an X-ray proportional chamber was employed. Data with this pioneering solar axion device were

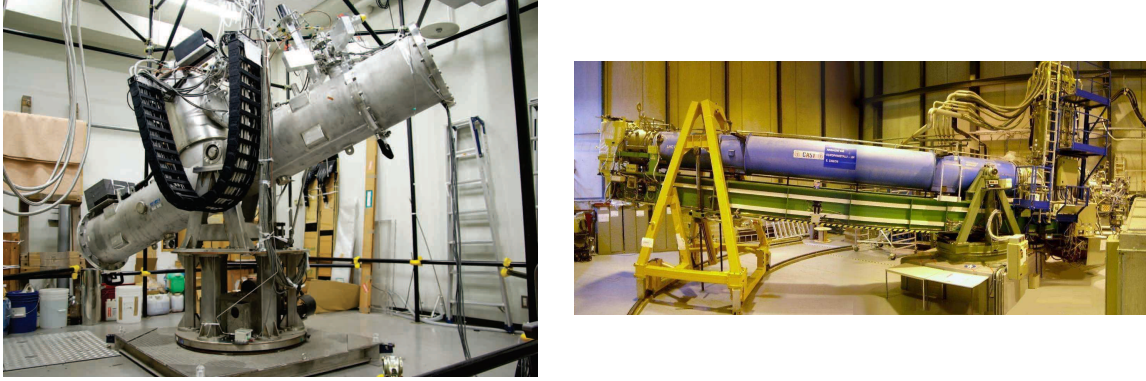


Figure 6. Recent pictures of the active axion helioscopes, Sumico on the left and CAST on the right.

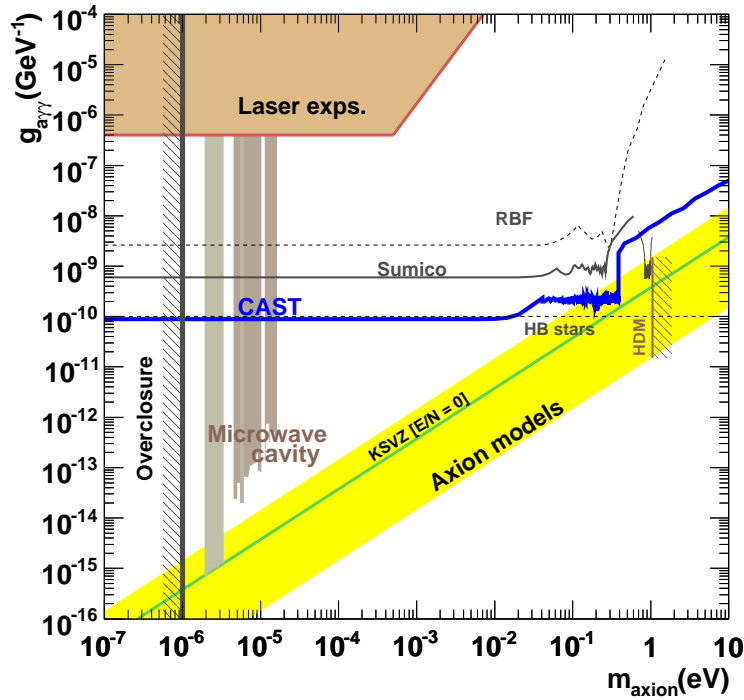


Figure 7. Exclusion plots in the axion-photon coupling versus the rest mass of the QCD-inspired axions. The limits achieved by helioscopes (RBF [25], Sumico [26–28], CAST [29–31]) are put in the general picture of the axion searches. For comparison are given the astrophysically and cosmologically derived conclusions: HB stars [56, 58], the hot dark matter limit (HDM) for hadronic axions $m_a < 1.05 \text{ eV}/c^2$ [57] inferred from WMAP observations of the cosmological large-scale structure, and the lower rest mass limit following overproduction of dark matter axions (overclosure of the Universe).

taken for about 4 h with the magnet pipe in vacuum and another 4 h with Helium buffer gas in the pipe in two different pressures. The results (Figure 7) were more sensitive than the laser experiments of that time by roughly two orders of magnitude, but still far from the theoretically motivated line (QCD axions).

5.2. The Tokyo helioscope (Sumico)

In 1997, in the University of Tokyo, a second generation axion helioscope took data, Sumico (Figure 6)[26]. A 2.3 m long magnet which reaches a field of 4 T, was mounted on a platform that enabled it to follow the Sun for approximately half a day (!). PIN photodiodes were used as X-ray detectors. Data were taken for one week with the magnet bores under vacuum conditions. The system was upgraded in 2000, when for one month measurements were taken with Helium gas in the magnetic pipes. When combining these two periods of measurement, an upper limit on the axion-to-photon coupling constant was derived for $m_a < 0.27 \text{ eV}/c^2$ [27]. Recently, the Sumico collaboration presented results for 34 mass settings around $1 \text{ eV}/c^2$. These measurements give the most stringent limit, so far, on the axion coupling for masses $0.84 < m_a < 1.00 \text{ eV}/c^2$ (Figure 7) [28].

5.3. The CERN Axion Solar Telescope (CAST)

CAST [29–31, 66] represents the third generation of axion helioscopes (Figure 6). In fact, it outscores the previous ones in many of the important parameters, starting with the key feature, the magnet, as can be seen in Table 1. It uses a decommissioned LHC prototype magnet which reaches a field of 9 T inside two parallel pipes of length 9.26 m and aperture 14.5 cm^2 each. This feature makes CAST the most sensitive helioscope built so far. The magnet is mounted on a moving platform which allows it to follow the Sun for approximately $2 \times 1.5 \text{ h}$ per day. Currently CAST uses 3 Micromegas X-ray detectors and an X-ray mirror optics coupled with a CCD camera at its focal plane (X-ray telescope). The latter system distinguishes CAST’s performance from any other axion helioscope (see section 4). The coherence condition restricts the CAST sensitivity to $m_a \leq 0.02 \text{ eV}/c^2$ when the magnetic pipes are under vacuum (Figure 3). The CAST result is, up to now, the most restrictive experimental limit on the axion-photon coupling constant for this mass range. Moreover, it competes with the previous astrophysical limit based on the Helium-burning lifetime of HB stars. Subsequently, CAST extended its sensitivity to $m_a \leq 0.4 \text{ eV}/c^2$ using ^4He inside the magnet pipes. Replacing the ^4He by ^3He , CAST can cover the axion rest mass range up to $\sim 1.2 \text{ eV}/c^2$.

According to (7), the sensitivity of an axion helioscope is determined by the following parameters: the strength of the magnetic field B , its length L , the effective axion-sensitive magnetic aperture A and the time of measurement t . Table 1 shows a comparison of the axion helioscopes based on these characteristics. The figure of merit, the product $(BL)^2$, which plays the most important role, is given in the first column. The next columns enhance the comparison with the additional information of the aperture and the axion exposure time. Sumico and CAST are the first ‘direct-search’ experiments that can probe the QCD axion model strip near the eV range in the $g_{a\gamma\gamma}$ - m_a parameter space.

Table 1. Comparison of figures of merit of the axion helioscopes. B is the strength of the magnetic field, L its length, A the effective, axion-sensitive magnetic aperture and t the tracking time per day (for the orbiting telescopes see [55, 71]).

Helioscope	$(BL)^2$ T ² m ²	$(BL)^2 A$ T ² m ⁴	$(BL)^2 At$ T ² m ⁴ hours
RBF	16	$\sim 3 \times 10^{-2}$	$\sim 1 \times 10^{-2}$
Sumico	85	$\sim 10 \times 10^{-2}$	$\sim 120 \times 10^{-2}$
CAST	6946	2000×10^{-2}	6000×10^{-2}
In orbit	324	20000×10^{-2}	–

5.4. Orbiting X-ray telescopes

The same working principle as the one of the above mentioned axion helioscopes can be applied with orbiting detectors sensitive to hard X-rays (see for example [72, 73] for the case of the RHESSI solar X-ray observatory, with a threshold above ~ 3 keV). Axion-to-photon conversion may occur either in the terrestrial magnetic field [71], or in the one near the solar atmosphere [55]. Despite the big differences between the two schemes, their sensitivity can compete with the best earth bound helioscope (see next section), but only for an axion rest mass range (far) below 10^{-4} eV/ c^2 . Furthermore, following the present article, solar X-ray telescopes in space may operate as the most sensitive solar axion antennas for more massive axions ($m_a > 10^{-3}$ eV/ c^2) by utilizing, complementarily, the solar magnetic fields near the photosphere. One is inclined to (Erroneously) consider such a scheme as an indirect method in axion helioscopy. The so obtained results can be equally significant, and eventually with a better built-in sensitivity, compared to the direct axion-detection techniques using axion helioscopes.

6. Photosphere: the resonant-coherent axion-photon converter?

In this second part, we move from the short man-made to large, natural occurring axion-photon converters near the solar surface. A rather large coherence length (> 1 -10 km) can be at work thanks to the low density and low Z solar gas. Indeed, in a specific layer of the continuously varying density, the resonance condition $\hbar\omega_{pl} \approx m_a c^2$ can restore coherence, provided the axion rest mass is above \sim meV/ c^2 . A first, rough comparison between the temperature of the solar plasma (~ 5800 K) and the well studied one of the infant Universe (Figure 8, upper left), of a rather similar temperature (~ 3000 K), is interesting due to the striking contrast between the perfect cosmic blackbody distribution and the equivalent one from the Sun (Figure 11). To put it differently: if the predicted and measured tiniest fluctuations of the cosmic plasma of $\Delta T/T \sim 10^{-5}$ provide(d) fundamental new physics, one is even more tempted to conclude that the unpredictable and huge solar atmospheric fluctuations ($\Delta T/T \sim 10^3$) might be the imprints of hidden new physics.

There is a fundamental difference between both plasmas under comparison: it

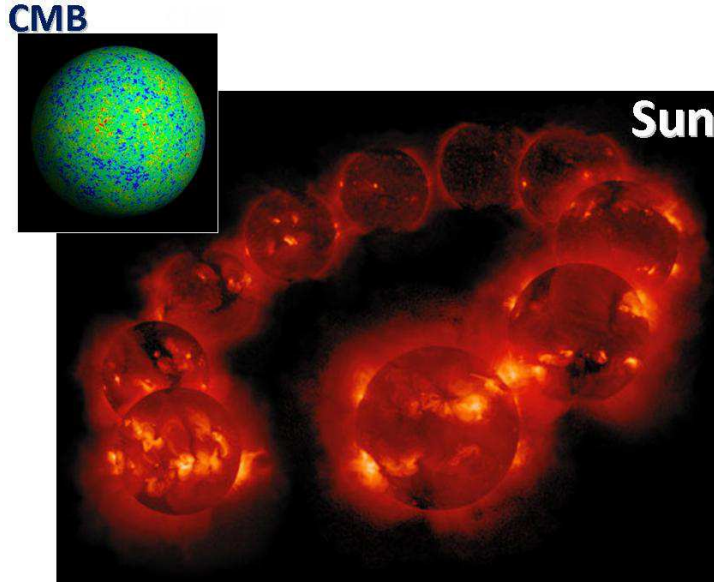


Figure 8. The changing brightness of the Sun in soft X-rays in different periods of its mysterious 11-year cycle was measured with the X-Ray Telescope of the Japanese Yohkoh mission (1991-2001). The solar atmospheric temperature fluctuations are huge ($\Delta T/T \sim 10^3$). The (quiet) Sun X-rays are conservatively unexpected, and this is the solar coronal heating problem (since 1939), which remains “*one of the most perplexing and unsolved problems in astrophysics to date*” [74]. For comparison, in the insert (upper left) the temperature fluctuations $\Delta T/T$ of the infant cosmic plasma are shown (at the 10^{-5} level, as they have been measured by WMAP). The temperature of both is similar: 5800 K versus 3000 K. One difference to be noticed is the quasi zero magnetic field in the cosmic plasma versus the varying solar magnetic fields in the Tesla scale. Remarkably, solar X-ray emission, above its steady component, follows spatio-temporally magnetic activity. Courtesy M. DiMarco/HAO & NCAR [75].

is only the solar plasma, which is permeated with unpredictable, huge-sized and \sim Tesla strong magnetic fields. Is this already a hint for axions, following the previous sections? We follow this simplified question in this second part of the article, which is observationally motivated.

6.1. General considerations

In the following, firstly, we suggest atypical solar axion signatures, even though the observed strong X-ray intensities cannot be reproduced rigorously within the QCD-inspired axion picture, i.e. only via the coherent inverse Primakoff effect; this is suggestive of other exotica with similar properties, or another axion-to-photon conversion process (our preference at present), or both. The Primakoff effect is at present the process behind the working principle of almost all axion experiments. Monte Carlo simulation has been performed, to follow the propagation of magnetically converted axions, that is, the created X-rays, near the solar surface. Secondly, we argue how puzzling solar behaviour can be the manifestation of axions, revising the so far widely accepted picture [55], which predicts a bright X-ray spot from coherently converted

pseudoscalars that can show-up only at the solar disk centre. The reasoning of this previous work is actually not wrong. We only arrive to different conclusions after comparing simulation results with solar X-ray observations which, since they originate from the whole magnetic surface, point tentatively rather at the photosphere or the (lower) chromosphere as the axion-to-photon conversion layer than the outer atmosphere as it was concluded in [55].

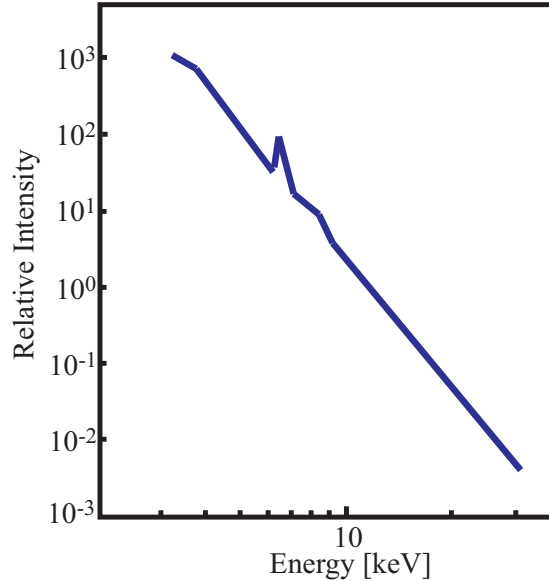


Figure 9. Qualitative drawing of the usually observed photon analog spectrum from solar activities like microflares (see also [77]). A similar trend towards lower energies has been observed above 0.8 keV very recently for the extreme quiet Sun [78].

Summarizing the previous sections we notice that axion helioscopes à la Sikivie [18] (e.g. the running Sumico and CAST [26–31]) utilize strong transverse macroscopic magnetic fields in order to force radiatively decaying particles, like the celebrated axions, to coherently transform to photons. This working principle raises the question as to whether and how it could have escaped one’s attention that axion conversion does happen already at the Sun’s *ubiquitous* surface magnetic fields. In fact, there are still conventionally unexplained solar phenomena, from the largest flares to the weakest transient or almost steady brightening (e.g. the hot solar corona), which are surprisingly associated with X-ray activity and solar magnetic fields. The primary process behind the X-ray flares, for a cool star like our Sun, is still missing [76]. Therefore, we follow such observations further, as possible candidates of solar axion signatures, which can be as direct as those earth bound helioscopes search for, but eventually more sensitive, for whatever reason. In the past, the various solar X-ray activities may not have been considered of axion origin, “simply” because:

- (i) the shape of any measured or reconstructed solar analog photon spectrum decreases rapidly with energy instead of showing at least a kind of a bump around 4-5 keV like in Figure 2 (see also Figures 9 and 10),

- (ii) the topology of the emitted X-rays does not resemble a spot-like structure that should be located at the solar disk centre covering $\sim 2\%$ of the solar disk [55]. If the coherent inverse Primakoff effect occurs far above the surface, there is a perfect collinearity between the outstreaming axion and the emerging photon. The axion source (=solar core), the intervening surface transverse magnetic field, and the Earth X-ray observer define a straight line ⁺. To put it differently, such axion related solar X-rays point away from the Earth, if their conversion place is OFF the solar disc centre,
- (iii) a signature from a dark matter particle candidate should be, by default, extremely faint.

Generally speaking, only if the above given three quasi prejudices against the axion involvement in the X-ray bright Sun can be overcome, will this revise the picture of our nearest star. Then, the huge sized solar surface magnetic fields should act, somehow, temporally as an efficient axion-to-photon catalyst due to a spatio-temporally occurring parameter fine-tuning. The question is, however, how does this happen? With Figure 3 in mind, a possibility would be if the plasma density of a sufficiently large volume, which is also sufficiently magnetized [24], is occasionally ‘tuned’ to the axion rest mass, enhancing the axion conversion efficiency. This could explain, in principle, some of the (transient) solar X-ray emission, in particular if its intensity shows a B^2 dependence, which seems to be often the case [84–86].

6.2. Axion(-like) signatures in solar observations

6.2.1. The hot corona

Following the above-mentioned three reasons, even the quiet Sun X-ray luminosity, which is the famous solar corona problem that has challenged astronomers since its discovery in 1939 by Walter Grotrian (Figures 10 and 11) ^{*}, should be naturally excluded from further consideration: the mean photon energy of the Sun’s corona is only about 100 eV (its temperature is a few MK), and its spectral shape is a steep exponential one (Figure 10). In addition, its birth place is not at all confined near the disk centre, but it covers the whole Sun (corona). Its intensity is only 10^{-7} of the solar luminosity, but still quite strong and easily observable. How the Sun

⁺ The solar disk centre was clearly distinguished in [55], i.e. axion related X-rays from the Sun should show up only near the disk centre. This is actually contrary to everyday experience with the solar X-ray data from the active and quiet Sun alike (Figure 13). The reasoning of [55] applies to low rest mass pseudoscalars with a relatively large coupling constant for a QCD-inspired axion, which are assumed to convert high in the upper chromosphere or beyond. Such a signature has been searched for since long time. The scenario of this article might give a reason for this non-observation. Both approaches do not contradict each other, since the axion rest mass is a crucial parameter ($m_a < 10^{-4} \text{eV}/c^2$ in [55], and $m_a > 10^{-3} \text{eV}/c^2$ in this work).

^{*} One should note that there is no short of reported solutions of the solar coronal heating problem. Indicatively, in the highly valued journal SCIENCE, the almost solution of the old puzzle has been announced twice [87], over a time interval of a decade, while concluding recently that “*the question of why the Corona is hot remains unanswered*”.

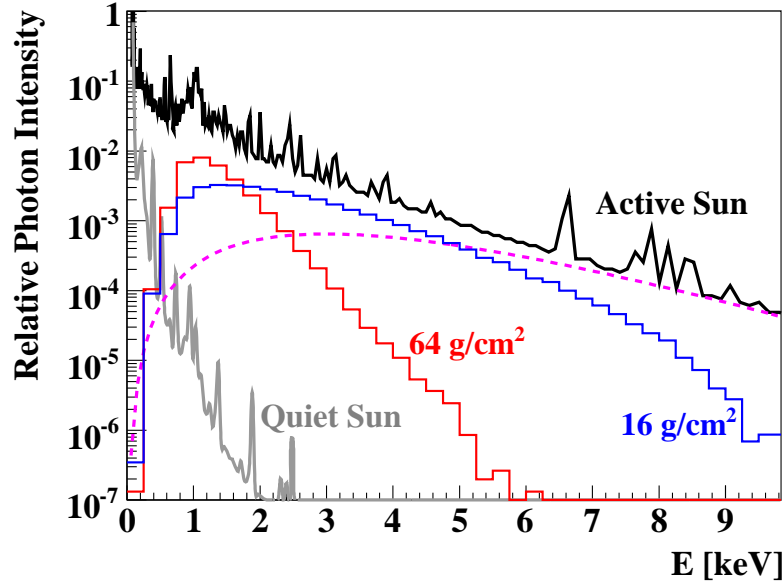


Figure 10. Reconstructed solar photon spectrum below 10 keV from the Active (flaring) Sun from accumulated observations (black line). Active Regions are associated with strong magnetic fields near the solar surface [79]. The dashed line is the converted solar axion spectrum. Two degraded spectra due to multiple Compton scattering are also shown for column densities above the initial conversion place of 16 g/cm^2 and 64 g/cm^2 , respectively, which actually agree with the observed spectral shape (simulated spectra are not to scale). The same interpretation picture could apply to the reconstructed spectrum of the non-flaring Quiet Sun at solar minimum (grey line), provided the conversion occurs deeper into the photosphere. This is also supported by the recent findings [79] that in the Quiet Sun regions stronger magnetic fields occur in deeper layers than in the Active Regions. The unknown energy source of the quiet Sun soft X-ray spectrum reflects the solar corona problem. Note, the Geant4 code photon threshold is at 1 keV (reconstructed solar photon spectra from [80]).

increases its temperature within a very short distance from 5800 K to a few MK (Figure 12) is the mystery behind the solar corona heating.

Previous axion work was motivated by the very steep transition region (Figure 12) separating the chromosphere and the corona [88–90]. It addressed the *steady* solar X-ray emission as coming from gravitationally trapped massive axions of the Kaluza-Klein type; their spontaneous decay near the Sun results to a self-irradiation of the whole solar atmosphere, which implies an inwardly directed radiation pressure. Along with X-rays expected to be emitted radially outwards from converted axions in magnetized places near the surface (see next), the balance between the two axion-related radiation pressures could explain otherwise nagging problems with the Transition Region (see also [91]), also reconciling results which contradict robust helioseismological data. For example, following the axion scenario, the anomalous elemental abundances can be only a surface effect, evading contradiction with the inner Sun properties.

Interestingly, the quiet Sun corona is hotter during solar maximum ($T \sim 2.2 \text{ MK}$) than during solar minimum ($T \sim 1.3 \text{ MK}$) [92]. This meets actually the reasoning of

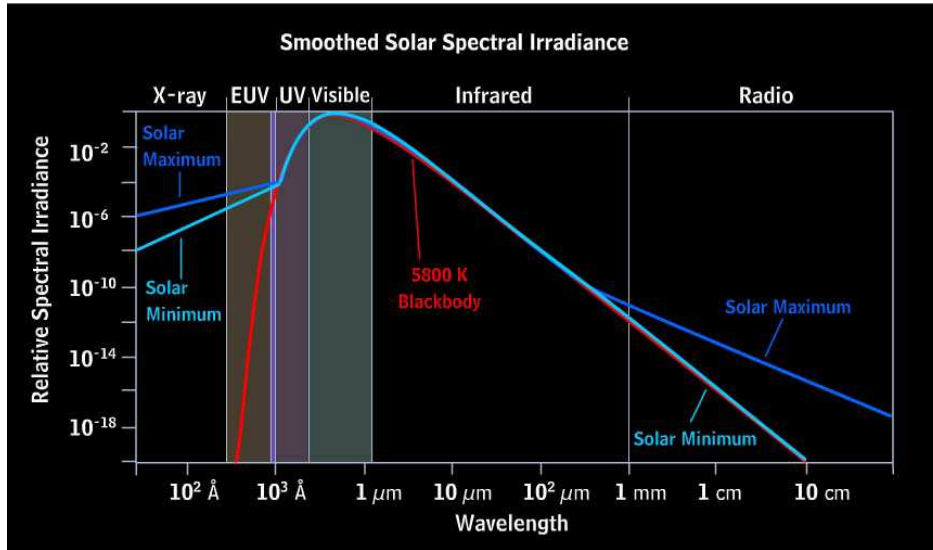


Figure 11. The solar irradiance spectrum for two periods in the 11-year sunspot cycle. The excess at low wavelengths (soft to hard X-rays) above the thermal distribution of a solar surface of 5800 K is conventionally unexpected (see also Figures 10 and 12). Courtesy M. DiMarco/HAO & NCAR [75].

this work, since the magnetic Sun follows the 11-year cycle and magnetically converted axions can in addition heat-up the atmosphere. More specifically, the solar corona above *non-flaring* Active Regions (ARs) reaches even flaring temperatures ($\sim 4\text{--}10$ MK) [93–96]. Remarkably, the AR corona can be largely heated to temperatures >5 MK only where the photospheric magnetic fields are the strongest [95]. In addition, the recent observation of a hot core ($T > 10$ MK) above a quiescent AR fits this work too [97].

6.2.2. Quiet Sun observations with RHESSI It is argued that the reported quiet Sun X-ray emission [98] in the 3–6 keV range, which is no longer considered as an upper limit ([73]), has been explained conventionally as the high energy tail of an X-ray emitting hot solar plasma. Alternatively, following the axion scenario of this work, the suggested spectral degradation for the flaring Sun (see MC simulations below) could be at work even stronger in the quiet Sun, which implies lower energy escaping photons due to enhanced Compton scattering (Figure 10). Recently, it has been observed that the stronger the surface magnetic field, the smaller the magnetic effects in the deeper layers and *vice versa* [79]. Then the extrapolation to higher energies will be different between the assumed thermal distribution [77] and the one following the squeezed axion-related X-ray spectrum towards low energies (this work).

6.2.3. Extreme Quiet Sun observations with SphinX The recently launched space mission with the SphinX detectors has already provided the first (preliminary) light curves in soft X-rays ($E_\gamma > 0.8$ keV) for extreme quiet Sun conditions [78]. The observed power-law spectral shape resembles, at least qualitatively, the corresponding one given

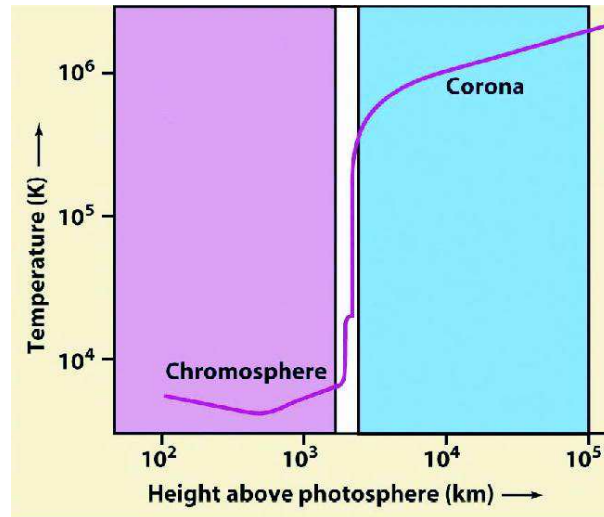


Figure 12. Atmospheric temperature distribution near the solar surface. The very existence of the \sim MK hot solar corona has challenged astronomers since its discovery in 1939 by Walter Grotrian [81]. Ironically, the Sun’s interior is better understood than its outer atmosphere. Why the temperature is rising in this way is one of the most challenging questions in astrophysics. Also the heating of the chromosphere [82] is a long-standing puzzle in solar physics. Courtesy M. Weinberg/University of Massachusetts [83].

in Figure 10 (grey line). Also this observation fits the axion scenario, and we consider it -at least- as an additional, independent piece of experimental evidence from the quiet Sun at its present 11-year minimum phase. The estimated X-ray luminosity above 0.8 keV is $\sim 5 \times 10^{21}$ erg/s. Extrapolating the measured spectrum [78] towards lower energies (grey line of Figure 10), the total soft X-ray luminosity becomes $\sim 5 \times 10^{24}$ erg/s $\simeq 10^{-9}L_{\odot}$. Even if these excess X-rays (from both RHESSI and SphinX [78, 98]) are due to a thermal distribution, e.g, from a ~ 10 MK plasma, the question about the origin of its actual heating source remains, since this is just the solar corona problem. Combining the energy distribution and the topology of the excess events will allow to distinguish between diffuse [88, ?, 90] and transient brightenings (this work).

6.2.4. Solar 2D spectra with YOHKOH/XRT In addition to the mentioned quiet Sun steady X-ray luminosity [78, 98], a further enhanced solar X-ray activity (at all levels) is occasionally observed, which is spatio-temporally correlated with the solar magnetic activity, and covers a relatively wide band in solar latitude ($\pm 35^{\circ}$). Both magnetic and X-ray activity appear equally in all longitudes between the west and east solar limb (Figure 13), with no trace of an enhanced activity near the disk centre [55]. A solar axion scenario must account for the surface topology of the X-ray distribution and the power-law spectral shape; the bulk of the emitted intensity is in soft X-ray emission, in agreement with this work (see below). Recent observations by the HINODE mission

found that the quiet Sun consists of a network of horizontal magnetic fields [101]. This makes then also the quiet Sun a potential axion-to-photon coherent converter, which gives rise to the observed soft X-rays surface distribution (Figures 13 and 10). Taking into account that the observed soft X-ray luminosity of the extreme quiet Sun [78] is $\sim 10^{-9}L_{\odot}$, there is no need to invent any enhancement factors as required for the largest flares (see section 6.3). One can always distinguish, however, between a diffuse contribution and individual X-ray sources from magnetic places.

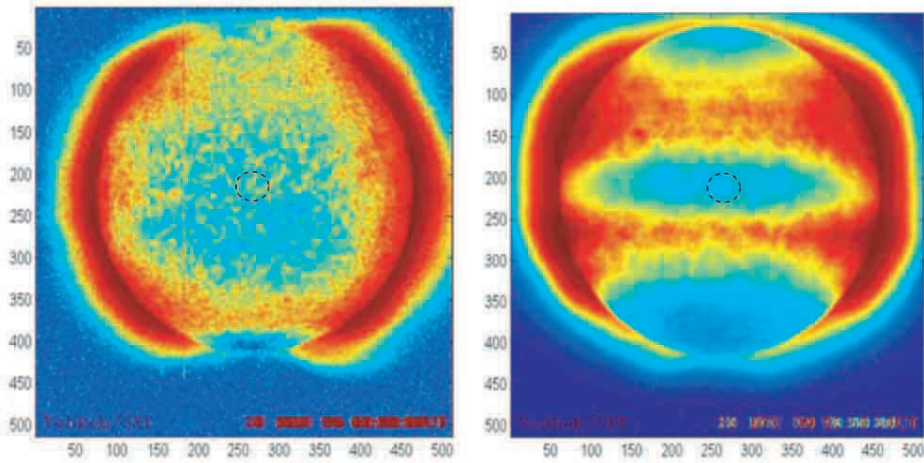


Figure 13. Solar images at photon energies from 250 eV up to a few keV from the Japanese X-ray telescope Yohkoh (1991–2001). The following is shown: On the left, a composite of 49 of the quietest solar periods during the solar minimum in 1996. On the right, solar X-ray activity during the last maximum of the 11-year solar cycle. The drawn circles indicate the region of the expected X-ray brightening spot near the disk centre, according to [55]. Both images show no sign of an X-ray bright spot at the disk centre (see text and [55]). On the contrary, most of the X-ray solar activity (right) occurs at a wide bandwidth of $\pm 35^\circ$ in latitude, being homogeneous in longitude. Note that $\sim 95\%$ of the solar magnetic activity covers this bandwidth [99] (see also a similar topology for microflares measured with RHESSI [100]). This X-ray topology matches this work for a ~ 10 meV/ c^2 solar axion or axion-like particle involvement.

6.3. First estimates

If one takes the experimentally derived upper limits for the axion-to-photon coupling strength (see e.g. [31]), a solar X-ray luminosity from converted QCD-inspired axions should be around 20 orders of magnitude below that of the visible Sun (3.8×10^{33} erg/s), i.e. extremely small. Therefore, to explain (large) X-ray flares, whose trigger remains a mystery, an enhancement by as much as $\sim 10^9$ is required, even under favourable conditions (see footnote ||). In other words, an unforeseen mode of interaction remained unnoticed so far, avoiding in this way any contradiction with observationally derived couplings, by ADMX, CAST and Sumico. As an example, we mention the concept suggested by Guendelman [102] about the axion interaction with magnetic field and

field *gradients*‡. This field configuration has never been taken into account in an axion experiment previously, at least not a priori. Surprisingly, solar X-ray activity is associated with places of strong magnetic field gradients [104]. Then, both the actual interaction and the very nature of the solar exotica in question may be different from the -otherwise inspiring- QCD axions. To put it differently, it is not improbable that we are not yet aware of every process occurring in the Sun, which goes beyond our standard solar axion picture and we may have not predicted yet all relevant particle candidates. Remarkably, as we subsequently show, the actual solar X-ray spectral shape and emission topology, resemble the standard solar axion scenario (though strongly modified, only if a near to the photosphere magnetized layer is the axion-to-photon converter). All this might explain why such solar axion signatures remained overlooked for such a long time, as well as why space weather is unpredictable.

In this part of the article, we focus on the magnetic/X-ray active Sun. In spite of the otherwise completely unfavourable observational picture for axions, following the reasoning of [55], we aim to explain how the solar axion scenario does apply. This will also allow to explain how such unnoticed solar signals for axions could leave the X-ray Sun covered with a veil of mystery since decades. The reader should know that although we are not solar experts, it is encouraging that solar X-ray missions like RHESSI and HINODE have implemented axions in their work [73]. Then, the insisting enigmatic behaviour of the Sun leaves room for novel and exotic phenomena. Solar X-ray observatories including YOHKOH a posteriori are the novel axion helioscopes in space, thus opening new windows of opportunity.

7. Isotropic X-ray emission from converted solar axions (simulation)

A simulated propagation of converted axions to X-rays near the photosphere has been performed. The novelty is that magnetically converted axions can be visible even from the whole solar disk for an Earth X-ray observer. Moreover, the measured analog photon spectrum can, naturally, be completely different from the original axion spectrum, being shifted towards lower energies. Remarkably, all expectations derived from the

‡ At the solar surface, we have the appearance of magnetic flux tubes, whose diameter is taken 100 km and the length some thousands of km. The interior magnetic field is taken to be 0.2 T. These tubes resemble the geometry of a solenoid. For this simple geometry recently [after submission of this article] E. Guendelman [103] has performed a calculation for the conversion probability of axions to photons, if they enter perpendicularly to the axis of the solenoid. Surprisingly, the conversion probability for such a solar flux tube is of the order of 50%. More interestingly, if instead of 100 km, one takes a diameter equal to 10 km and 1 km, the conversion probability drops to $\sim 10^{-2}$ and $\sim 10^{-6}$, respectively. Needless to say, also these last two conversion probabilities are still very large, compared to the estimated yield of 10^{-12} (see footnote ||). Note that there are many such flux tubes at the Sun, which may explain a very wide band of solar X-ray emission. In addition, if plasma resonance effects are required, in order to enhance the conversion probability, coherence lengths of ~ 1 to 10 km are actually reasonable to consider for the active Sun, taking as reference the static density distribution below the solar surface. These estimates may show how the next generation axion magnetic helioscopes (and haloscopes?) will look like.

Monte Carlo simulation fit solar X-ray observation (Figures 9, 10 and 13). In fact, the depth of the actual conversion region is the only ‘free’ parameter, which can be derived individually or through combining: the slope (=power law index) of the X-ray spectrum, the spatial extension of the emitting region, and the mean photon energy. Statistically, also the obtained degree of erasure of the initial photon directivity is dependent on the axion conversion depth in the photosphere (Figure 14).

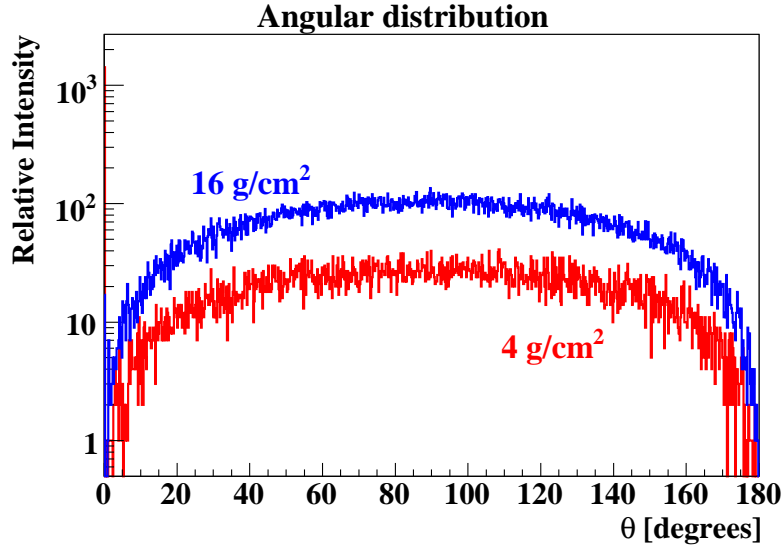


Figure 14. Simulation with the CERN / Geant4 code. The angular distribution of X-rays from converted solar axions inside the magnetized solar surface for two atmospheric column densities above the axion-conversion place is given. The photoelectric effect has been inactivated, thus resembling free plasma electrons. The initial radial axion trajectory direction is taken at $\Theta=0^\circ$. In a vacuum, all solar X-rays from the assumed inverse Primakoff effect would also escape at $\Theta=0^\circ$. Simulated converted axion events $N_0=16415$. Number (N) of not interacting X-rays at $\Theta=0^\circ$: $N=1422$ or 8.7% for 4 g/cm^2 , and $N=18$ or 1.1‰ for 16 g/cm^2 .

7.1. A qualitative estimate

In order to divert an X-ray in the $\sim 1\text{-}10\text{ keV}$ energy range from its collinear direction of propagation with the converted axion trajectory, one or even the only possibility is via the isotropic Compton scattering. For this to happen, a thick plasma above the axion conversion place is required, suppressing the photoelectric effect. In fact, also a self-photoionization can start with converted axion-like exotica near the magnetized solar sub-surface, which can irradiate and transform an overlying neutral layer to a plasma. Appropriate environmental conditions, e.g. plasma density resonance effects over extended regions, can considerably enhance the axion interaction. ††

††If converted axions are the only source of ionization, this might last for some time. The estimated time to photoionize, e.g. $\sim 2\text{ g/cm}^2$ above the flare trigger place is of the order of 10^3 s , assuming an integrated axion originated solar X-ray surface brightness of $10^{-2}L_\odot$ to be the energy source. This

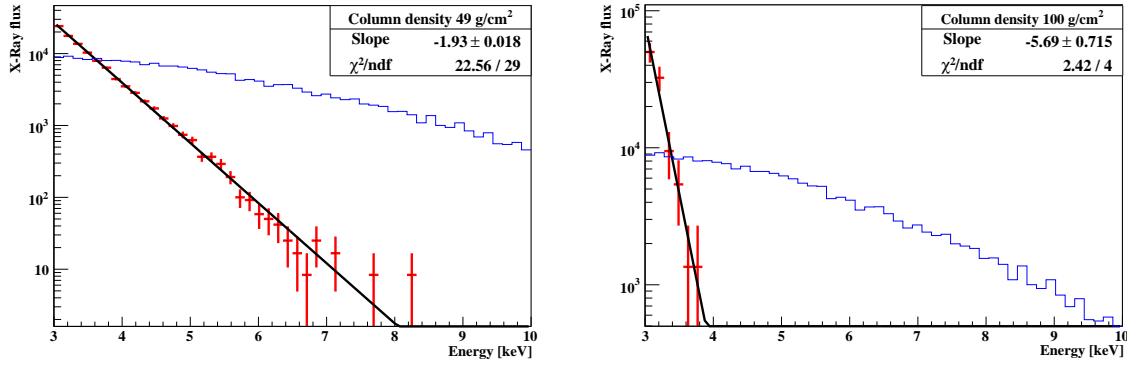


Figure 15. Simulation of the non-linear energy degradation due to multiple Compton scattering of hard X-rays, which start inside the photosphere with a solar plasma column density above 49 g/cm^2 (left) and 100 g/cm^2 (right). The initial energy distribution (thin line histogram in blue) is that of the solar axion spectrum (Figure 2). The strong change of the initial analog spectrum depends on the photon's random path. The steepness of the distributions depends sensitively on the initiation depth, i.e. on the axion-to-photon conversion place, where the otherwise unexpected X-rays are assumed to be emitted radially outwards inside the relatively cool photosphere ($T < 10000 \text{ K}$). For the same density, the depth can vary in the dynamic Sun. Surprisingly, these otherwise colourless spectral shapes reflect solar observations (Figures 9, 10), with the emitted photon spectra dominating exponentially towards lower energies (see also Figure 16).

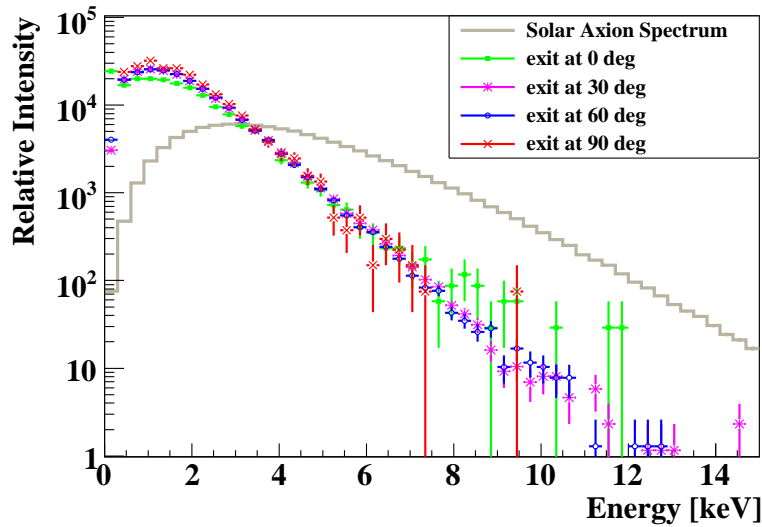


Figure 16. The same as in Figure 15, assuming the X-rays are created at a depth of 500 km into the photosphere. This Monte Carlo simulation shows that the shape of the expected analog spectrum does not depend on the relative angle of observation, which is actually counterintuitive. Note, that the Geant4 photon threshold is at 1 keV , and therefore the turndown around $\sim 1 \text{ keV}$ is an artefact.

requirement is in principle possible, even though extreme (however, the appearance of a large solar flare is also an extreme and relatively rare event). It cannot be excluded that some other conventional

In any case, a more or less bright X-ray flaring region, whatever the trigger process, remains as a fully ionized plasma until it starts cooling down to ambient pre-flaring temperatures. X-rays from converted exotica undergo Compton scattering with the surrounding plasma electrons. A scattering probability [107], say, of about 50%, requires an (ionized) column density of 1-2 g/cm². Surprisingly, such column densities do exist near the solar surface. For example, some column densities for the static Sun are [108]: a) ~ 4.4 g/cm² at the surface of the photosphere increasing rapidly underneath, and b) ~ 1 g/cm² and $\sim 10^{-3}$ g/cm² at +200 km and +1000 km into the chromosphere, respectively. Note that the plasma density in the solar corona changes dynamically by a factor of 10-100 at any given time [109]; this actually holds, at a lower degree, for both chromosphere and photosphere [110]. This implies that the isotropic Compton scattering of X-rays from converted axions occurring even higher in the atmospheric plasma can still be quite considerable, i.e. it might happen even at larger heights than those anticipated for the static atmosphere.

Consequently, if the actual flaring trigger place is (far) below the Transition Region (Figure 12), the initially radially and outwardly emitted X-rays from outstreaming and converted axions can keep the intervening neutral gas above ionized. It is simply this plasma above the actual flaring trigger place, which acts as the intervening Compton X-ray scatterer. Thus, a kind of a dynamic ‘solar surface effect’ can be at work, whose thickness is only of the order of 1000 km across the solar surface. Then, it is this thin layer underneath and above the photosphere surface, which is ‘distinguished’ within our axion approach, since it allows for a self-tuning that enhances the axion conversion, provided $m_\gamma = m_a \sim 10^{-2}$ eV/c². The disk centre region for axions with such a rest mass is no more peculiar as it was concluded for very light pseudoscalars in [55]. In the past ~ 13 years, the conclusions from [55] might have been misleading the axion ID in solar X-rays. Axions with $m_a \gtrsim 10^{-2}$ eV/c² result finally to an isotropic X-ray emission, due to the intervening Compton scatterer, which makes the whole magnetized solar disk a potential axion-to-photon converter, visible to an outside observer (Figure 13).

7.2. Monte Carlo Simulation

In the simulation with the CERN Geant4 code, the photoelectric effect was inactivated in order to mimic the propagation of X-rays in a thick plasma ($> \text{few g/cm}^2$), which after (multiple) scattering and a ‘random walk’ escape into free space. The derived isotropic X-ray re-emission from this simulation for two column densities (Figure 14) supports quantitatively the basic idea behind this work. This means that the information about

reaction mechanism is in synergy, like the celebrated reconnection of opposite magnetic fields. This implies a magnetic field gradient across the neutral line, which is, surprisingly, linked to solar X-ray activity. In the quiet Sun, only the tiny layer below the transition region to the deep photosphere is actually not fully ionized. Moreover, even for large X-ray flares, the surface brightness does not actually exceed the quiet Sun luminosity. The flare region is heated up to 10-30 MK [104, 106], remarkably close to that of the core $\sim 700\,000$ km underneath. Within the so defined solar axion ID, the X-ray sun reveals its otherwise hidden face.

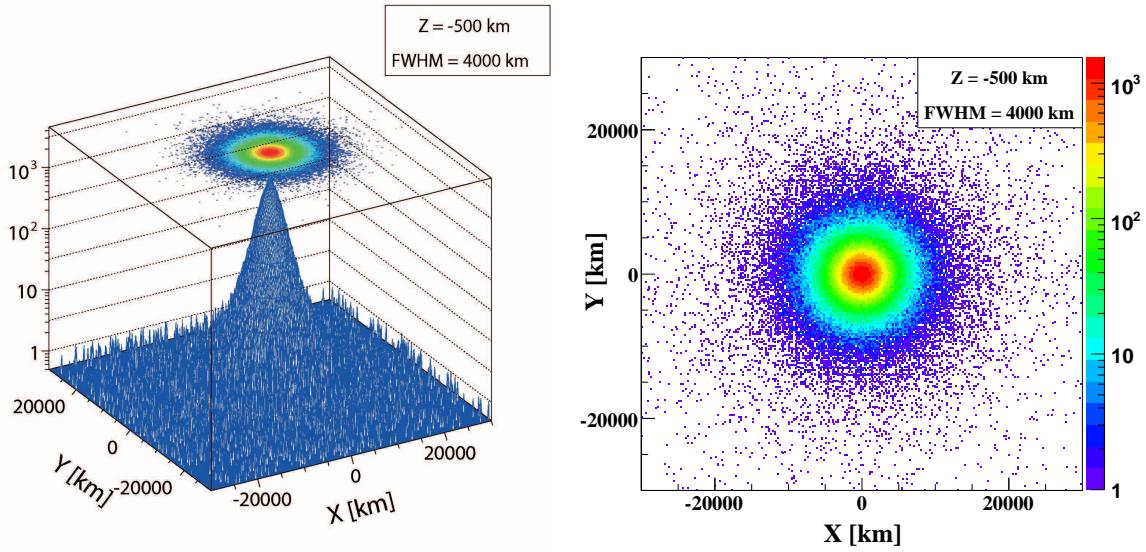


Figure 17. 2D and 3D shower development simulation of an initial pencil-like beam of hard X-rays that started at a depth of 500 km underneath the solar surface. Their initial energy distribution resembles that of the solar axion spectrum (Figure 2). When they escape from the solar surface after many Compton scattering in a random walk, they give rise to a characteristic lateral distribution, which resembles that of a microflare (see [105]). Combining this information with their spectral shape (see Figures 15 and 16), the initial place of the X-rays can be constrained.

the direction of the initial axion trajectory, which is transferred entirely to the first photon emerging in the coherent inverse Primakoff effect, is already erased with the very first Compton scattering.

In addition, in the same Monte Carlo simulation, we have also studied the photon energy degradation. The next surprising results are shown in Figures 10, 15 and 16. The original X-ray spectrum undergoes a tiny but non-linear energy redshift after each Compton scattering due to the energy dependence defined by the Compton kinematics. This is the reason behind the resulting power law spectral shapes, as they are given in Figures 15 and 16, being strikingly similar to those observed from active and quiet Sun alike (Figures 9 and 10).

To cross-check the suggested axion scenario, Figure 17 shows the statistical 3D and 2D ‘shower’ development accumulating many X-ray events; their initial energy distribution was taken to follow the shape of the standard solar axion spectrum (Figure 2). Interestingly, the steepness of the spectrum of the escaping photons depends critically on the depth into the photosphere at which the axion-photon conversion originates. The plasma density at the initiating conversion place provides input on the axion rest mass (Figure 3). In addition, within the axion scenario of this work, the spatial extension of the escaping X-rays (Figure 17) allows as well to independently derive the depth at which the propagation of the initial X-rays have started. At the current stage of this work, it is also encouraging that the derived surface size (Figure 17) fits observations with microflares (Figure 3 in [105]). This additional feature in favour

of the axion scenario supports this work, even though no firm conclusion can be derived on the role of the magnetic field B , or the magnetic field gradient $\partial B/\partial z$, or both.

8. Conclusions and Outlook for the Future

The present status and the performance of the two operational state-of-the-art axion helioscopes (Sumico and CAST), including their possible future upgrades are discussed in this work. Both have the potential to *directly* detect solar axions or other exotica with similar properties in a mass range below $\sim 1\text{-}2\text{ eV}/c^2$. In the next 2-3 years, they will provide at least the best limits for the interaction of axions with matter, if: a) the incoherent Primakoff effect is the main source of axion creation inside the hot solar core, and b) axions all stream freely out of the Sun isotropically, reaching the earth bound magnetic helioscopes when they are pointing at the Sun.

In addition, we studied whether the working principle of the axion helioscopes applies already near the dynamic photosphere, but was unnoticed before. Since magnetic fields are ubiquitous in the outer Sun, and, partly -if not entirely- permeating the inner Sun, this suggested to reconsider solar data from the solar axion point of view of the present work. This has been done, arguing in particle physics manner, with the help of a Monte Carlo simulation of both the active/flaring and the quiet Sun. The considered solar observations can be reconciled with the axion scenario taking place near the solar surface. The derived rest mass for the axion(-like) particle is $m_a \sim 10\text{ meV}/c^2$, assuming that plasma resonance effects are at work near the photosphere. Then the photosphere itself or the near (lower) chromosphere is the actual catalyst for the axion conversion.

We note that magnetic fields are in the conventional picture somehow the energy reservoir for X-ray activity, but, in the axion scenario they are the self-catalyst for the axion-to-photon oscillation to occur, with the energy resources being outstreaming axions from the hot core instead. In reality, conventional and new physics might coexist, being complementary and not excluding each other. This makes it certainly more difficult to disentangle the axion contribution as an explanation of the solar activity [104, 111]. The magnetically created hard X-rays from axions undergo near the photosphere multiple Compton scattering, following an outwards random walk, whose non-linear energy loss dependence changes drastically the original spectral shape. Its properties like mean energy, steepness, lateral size, etc. have almost nothing in common with the conventionally expected solar axion picture, at least not at first glance. However, the striking similarities of the simulated features with the directly measured or the observationally reconstructed ones (Figures 9, 10, 13, 14), cannot be ignored, because the estimate of the X-ray emission, within the conventional solar axion scenario, is rather qualitative. After all, such or other exotica in question might interact via other channels, and/or their properties do not match that much the standard axions. A generic example for this to happen is certainly the suggested interaction of axions with magnetic field gradients. This scheme is supported by the solar observations which find that enhanced X-ray activity correlates not only with magnetic active regions (sunspots),

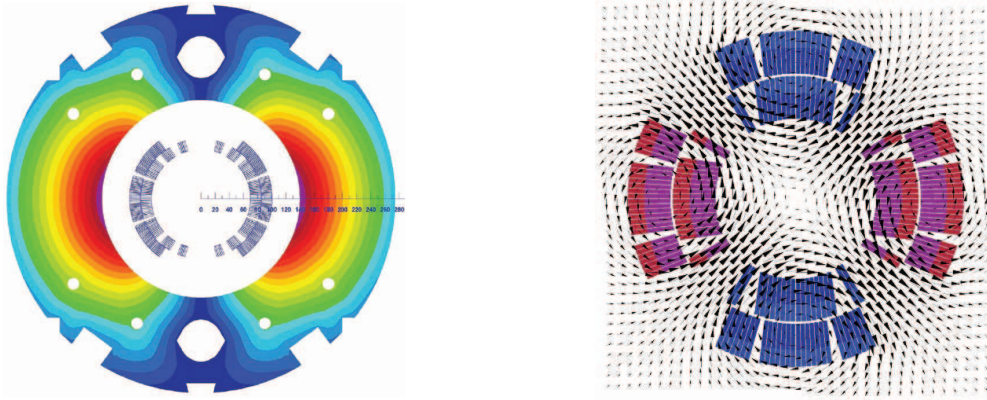


Figure 18. New magnets for an upgraded axion helioscope. Left: a magnet dipole, 16 m long, with 9 T and 140 mm aperture. Right: a quadrupole magnet with a maximum magnetic field of ~ 10 T and magnetic field gradient up to ~ 2.5 T/cm (see text). Courtesy: Stephan Russenschuck / CERN.

but also with places with magnetic field gradients [112, 113].

If an overlooked novel mode of conversion occurs, e.g. in magnetic field gradients, this avoids contradiction between the present limits on the axion coupling strength and the observed level of solar X-ray emission from magnetized places, since all magnetic axion detectors use instead dipole fields. Therefore, a future upgrade of present axion helioscopes implies a larger and more powerful magnet (Figure 18), lowest noise detectors, focusing devices, and much lower energy threshold. Inspired by the solar X-ray activity observations, some first measurements with quadrupole magnets (Figure 18) are in place, leaving room for surprises.

Acknowledgments

We would like to thank the referees for the constructive comments and criticism over this paper; we do believe that following their recommendations, this paper has gained in clarity and (scientific) value. We are thankful to the members of the CAST collaboration, for the use of CAST related results. Similarly, we also thank professor Makoto Minowa from the Sumico collaboration. We gratefully acknowledge the support of Biljana Lakić and Magda Lola. One of us (K.Z.) thanks Hugh Hudson for informative discussions during his short visit at CERN. We thank Tullio Basaglia from the CERN library for providing promptly most of the publications used throughout this work. K.Z. thanks CERN for long years of hospitality and support of all kind. We give credit to Eduardo Guendelman for allowing us to use the conversion probabilities he has calculated prior to publication. The support we have received from the Greek funding agency GSRT is gratefully acknowledged. This research was partially supported by the ILIAS (Integrated Large Infrastructures for Astroparticle Science) project funded by the EU under contract EU-RII3-CT-2004-506222.

References

- [1] Komatsu E et al. [WMAP Collaboration] 2009 *ApJ. SUPPL* **180** 330-376 [arXiv:astro-ph/0803.0547]
- [2] Baluni V 1979 *Phys. Rev. D* **1** 2227-2229
- [3] Crewther R J, Di Vecchia P, Veneziano G and Witten E 1979 *Phys. Lett. B* **88** 123
Crewther R J, Di Vecchia P, Veneziano G and Witten E 1980 (*E*) *Phys. Lett. B* **91** 487
- [4] Khriplovich I B, Korkin R A 2000 *Nucl. Phys. A* **665** 365
- [5] Lebedev O, Olive K A, Pospelov M and Ritz A 2004 *Phys. Rev. D* **70** 016003
- [6] Pospelov M, Ritz A 2005 *Ann. Phys.* **318** 119.
- [7] Liu C P and Timmermans R G E 2004 *Phys. Rev. C* **70** 055501.
- [8] Baker C A, Doyle D D, Geltenbort P, Green K, van der Grinten M G D, Harris PG, Iaydjiev P, Ivanov S N, May D J R, Pendlebury J M, Richardson J D, Shiers D and Smith K F 2006 *Phys. Rev. Lett.* **97** 131801.
- [9] Peccei R D and Quinn H R 1977 *Phys. Rev. Lett.* **38** 1440
- [10] Peccei R D and Quinn H R 1977 *Phys. Rev. D* **16** 1791
- [11] Peccei R D 2008 The strong CD problem and axions *Axions: Theory, Cosmology, and Experimental Searches (Lect. Notes Phys. vol 741)* ed M Kuster, B Beltran and G Raffelt (Berlin Heidelberg: Springer) p 3
- [12] Weinberg S, 1978 *Phys. Rev. Lett.* **40** 223
- [13] Wilczek F, 1978 *Phys. Rev. Lett.* **40** 279
- [14] Kim J E 1979 *Phys. Rev. Lett.* **43** 103
- [15] Shifman M A, Vainshtein A I and Zakharov V I 1980 *Nucl. Phys. B* **166** 493
- [16] Dine M, Fischler W and Srednicki M 1981 *Phys. Lett. B* **104** 199
- [17] Zhitnitskii A R 1980 *Yad. Fiz.* **31** 497
Zhitnitskii A R 1980 *Sov. J. Nucl. Phys.* **31** 260 (translation)
- [18] Sikivie P, 1983 *Phys. Rev. Lett.* **51** 1415
Sikivie P 1984 (*E*) *Phys. Rev. Lett.* **52** 695
- [19] Bradley R, Clarke J, Kinion D, Rosenberg L J, van Bibber K, Matsuki S, Mück M and Sikivie P 2003 *Rev. Mod. Phys.* **75** 777
- [20] Haggmann C, Kinion D, Stoeffl W, van Bibber K, Daw E, Peng H, Rosenberg L J, LaVeigne L, Sikivie P, Sullivan N, Tanner D, Nezhick D, Turner M S, Moltz D, Powell J and Golubev N 1998 *Phys. Rev. Lett.* **80** 2043 [astro-ph/9801286]
- [21] Asztalos S J, Bradley R F, Duffy L, Haggmann C, Kinion D, Moltz D M, Rosenberg L J, Sikivie P, Stoeffl W, Sullivan N S, Tanner D B, van Bibber K and Yu D B 2004 *Phys. Rev. D* **69** 011101 [astro-ph/0310042]
- [22] Duffy L, Sikivie P, Tanner D B, Asztalos S, Haggmann C, Kinion D, Rosenberg L J, van Bibber K, Yu D and Bradley R F 2005 *Phys. Rev. Lett.* **95** 091304 [astro-ph/0505237]
- [23] Asztalos S J, Rosenberg L J, van Bibber K, Sikivie P and Zioutas K 2006 *Ann. Rev. Nucl. Part. Sci.* **56** 293-326
- [24] van Bibber K, McIntyre P M, Morris D E and Raffelt G G 1989 *Phys. Rev. D* **39** 2089
- [25] Lazarus D M, Smith G C, Cameron R, Melissinos A C, Ruoso G, Semertzidis Y K and Nezhick F A 1992 *Phys. Rev. Lett.* **69** 2333
- [26] Moriyama S, Minowa M, Namba T, Inoue Y, Takasu Y and Yamamoto A 1998 *Phys. Lett. B* **434** 147-152 [hep-ex/9805026]
- [27] Inoue Y, Namba T, Moriyama S, Minowa M, Takasu Y, Horiuchi T and Yamamoto A 2002 *Phys. Lett. B* **536** 18-23 [astro-ph/0204388]
- [28] Inoue Y, Akimoto Y, Ohta R, Mizumoto T, Yamamoto A and Minowa M 2008 *Phys. Lett. B* **668** 93-97 [arXiv:0806.2230v2 [astro-ph]]
- [29] Zioutas K et al (CAST Collaboration) 2005 *Phys. Rev. Lett.* **94** 121301 [hep-ex/0411033]
- [30] Andriamonje S et al (CAST Collaboration) 2007 *J. Cosmol. Astropart. Phys.* JCAP04(2007)010

- [hep-ex/0702006]
- [31] Arik E *et al* [CAST Collaboration] 2009 *J. Cosmol. Astropart. Phys.* JCAP02(2009)008 [arXiv:0810.4482v2 [hep-ex]]
- [32] Paschos E A and Zioutas K 1994 *Phys. Lett. B* **323** 367
- [33] Avignone III F T, Abriola D, Brodzinski R L, Collar J I, Creswick R J, DiGregorio D E, Farach H A, Gattone A O, Guerard C K, Hasenbalg F, Huck H, Miley H S, Morales A, Morales J, Nussinov S, Ortiz de Solorzano A, Reeves J H, Villar J A and Zioutas K (The SOLAX Collaboration) 1998 *Phys. Rev. Lett.* **81** 5068 [astro-ph/9708008]
- [34] Morales A, Avignone III F T, Brodzinski R L, Cebrian S, Garcia E, Gonzalez D, Irastorza I G, Miley H S, Morales J, Ortiz de Solorzano A, Puimedon J, Reeves J H, Sarsa M L, Scopel S and Villar J A 2002 *Astropart. Phys.* **16** 325 [hep-ex/0101037]
- [35] Bernabei R, Belli P, Cerulli R, Montecchia F, Nozzoli F, Incicchitti A, Prosperi D, Dai C J, Hec H L, Kuang H H, Mac J M and Scopel S 2001 *Phys. Lett. B* **515** 6
- [36] Maiani L, Petronzio R and Zavattini E 1986 *Phys. Lett. B* **175** 359
- [37] Raffelt G and Stodolsky L 1988 *Phys. Rev. D* **37** 1237
- [38] Cameron R, Cantatore G, Ruoso G, Semertzidis Y, Halama H J, Lazarus D M, Prodell A G, Neziric F, Rizzo C and Zavattini E 1993 *Phys. Rev. D* **47** 3707
- [39] Zavattini E, Zavattini G, Ruoso G, Polacco E, Milotti E, Karuza M, Gastaldi U, Di Domenico G, Della Valle F, Cimino R, Carusotto S, Cantatore G and Bregant M (PVLAS Collaboration) 2006 *Phys. Rev. Lett.* **96** 110406 [hep-ex/0507107]
- [40] Ringwald A 2003 *Phys. Lett. B* **569** 51 [hep-ph/0306106]
- [41] Rabadan R, Ringwald A and Sigurdson K 2006 *Phys. Rev. Lett.* **96** 110407 [hep-ph/0511103]
- [42] Kötzig U, Ringwald A and Tschentscher T 2006 Production and detection of axion-like particles at the VUV-FEL: Letter of intent DESY 06-098 *Preprint* arXiv:hep-ex/0606058v1
- [43] Lindner A, 2006 *Search for axion-like particles at DESY: The ALPS project* Talk given at *Axions at the Institute for Advanced Study* (20–22 Oct. 2006, IAS, Princeton, New Jersey), <http://www.sns.ias.edu/~axions>
- [44] Cantatore G 2006 *Probing the quantum vacuum with polarized light: Results and outlook from the PVLAS experiment* Talk given at *Axions at the Institute for Advanced Study* (20–22 Oct. 2006, IAS, Princeton, New Jersey), <http://www.sns.ias.edu/~axions>
- [45] Afanasev A V, Baker O K, McFarlane K W, Biallas G H, Boyce J R and Shinn M D 2006 Production and detection of very light spin-zero bosons at optical frequencies COSM-06-02 *Preprint* arXiv:hep-ph/0605250v4
- [46] Afanasev A 2006 *LIPSS project: A search for photon regeneration at optical frequencies* Talk given at *Axions at the Institute for Advanced Study* (20–22 Oct. 2006, IAS, Princeton, New Jersey), <http://www.sns.ias.edu/~axions>
- [47] Battesti R 2006 *The BMV project* Talk given at *Axions at the Institute for Advanced Study* (20–22 Oct. 2006, IAS, Princeton, New Jersey), <http://www.sns.ias.edu/~axions>
- [48] Pagnat P 2006 *Laser-based experiments in high magnetic field for QED test and axion search at CERN* Talk given at *Axions at the Institute for Advanced Study* (20–22 Oct. 2006, IAS, Princeton, New Jersey), <http://www.sns.ias.edu/~axions>
- [49] Sikivie P, Tanner D B and van Bibber K 2007 *Phys. Rev. Lett.* **98** 172002 [hep-ph/0701198]
- [50] Moriyama S 1995 *Phys. Rev. Lett.* **75** 3222.
- [51] Krčmar M, Krečak Z, Stipčević M, Ljubičić A and Bradley D A 1998 *Phys. Lett. B* **442** 38 [nucl-ex/9801005]
- [52] Namba T 2007 *Phys. Lett. B* **645** 398.
- [53] Krčmar M, Krečak Z, Ljubičić A, Stipčević M and Bradley D A 2001 *Phys. Rev. D* **64** 115016 [hep-ex/0104035]
- [54] Ljubičić A, Kekez D, Krečak Z and Ljubičić T 2004 *Phys. Lett. B* **599** 143 [hep-ex/0403045]
- [55] Carlson E D and Tseng L S 1996 *Phys. Lett. B* **365** 193
- [56] Raffelt G G 2008 Astrophysical axion bounds *Axions: Theory, Cosmology, and Experimental*

- Searches (Lect. Notes Phys. vol 741)* ed M Kuster, B Beltran and G Raffelt (Berlin Heidelberg: Springer) p 51
- [57] Hannestad S, Mirizzi A and Raffelt G, *J. Cosmol. Astropart. Phys.* JCAP07(2005)002 [hep-ph/0504059]
- [58] Raffelt G G 1996 *Stars as Laboratories for Fundamental Physics* (Chicago: The University of Chicago Press)
- [59] De Angelis A, Roncadelli M and Mansutti O 2007 *Phys. Rev. D* **76** 121301
- [60] De Angelis A, Mansutti O and Roncadelli M 2008 *Phys. Lett. B* **659** 847
- [61] Roncadelli M, De Angelis A and Mansutti O 2008 *AIP Conf. Proc.* **1018** 147-156 [arXiv:0902.0895v1 [astro-ph.CO]]
- [62] Simet M, Hooper D and Serpico P D 2008 *Phys. Rev. D* **77** 063001
- [63] Fairbairn M, Rashba T and Troitsky T 2009 Photon-axion mixing in the Milky Way and ultra-high-energy cosmic rays from BL Lac type objects - Shining light through the Universe *Preprint* arXiv:0901.4085v1 [astro-ph.HE]
- [64] Burrage C, Davis A C, Shaw D J 2009 *Phys. Rev. Lett.* **102** 201101 [arXiv:0902.2320v1 [astro-ph.CO]]
- [65] DiLella L, Pilaftsis P, Raffelt G G and Zioutas K 2000 *Phys. Rev. D* **62** 125011
- [66] Cantatore G *et al* 2008 *Proc. 4th Patras Workshop on axions, WIMPs, WISPs* DESY, Hamburg, Germany, 16-21 June 2008 *Preprint* arXiv:0809.4581v2 [hep-ex]
- [67] Raffelt G G 1986 *Phys. Rev. D* **33** 897
- [68] Couvidat S, Turck-Chieze S and Kosovichev A G 2003 *ApJ.* **599** 1434
- [69] Livingston W, Harvey J W, Malanushenko O V and Webster L 2006 *Sol. Phys.* **239** 41
- [70] Creswell R J, Nussinov S and Avignone III F T 2008 *Phys. Rev. D* **78** 017702
- [71] Davoudsial H and Huber P 2006 *Phys. Rev. Lett.* **97** 141302
- [72] Hannah I G, Hurford G J, Hudson H S, Lin R P 2007 *Rev. Sci. Instrum.* **78** 024501
- [73] Hannah I G, Hurford G J, Hudson H S, Lin R P, van Bibber K 2007 *ApJ.* **659** L77
- [74] Antolin P, Shibata K, Kudoh T, Shiota D and Brooks D 2009 Signatures of Coronal Heating Mechanisms To appear in *Magnetic Coupling between the Interior and the Atmosphere of the Sun*, eds. S S Hasan and R J Rutten, Astrophysics and Space Science Proceedings (Springer-Verlag: Heidelberg, Berlin) *Preprint* arXiv:0903.1766v1 [astro-ph.SR]
- [75] Interactive courtesy of the COMET program and the High Altitude Observatory at NCAR (the National Center for Atmospheric Research).
http://www.windows.ucar.edu/tour/link=/sun/activity/solar_variation.html
- [76] Benz A O 2008 *Living Reviews in Solar Physics* **5** 1 (<http://www.livingreviews.org/lrsp-2008-1>)
- [77] Hannah I G, Christe S, Krucker S, Hurford G J, Hudson H S and Lin R P 2008 *ApJ.* **677** 704
- [78] Sylwester J 2009 *SphinX: aims, construction and first results* Talk in the Soteria Workshop, 23-24 March 2009, Saariselk, Finnish Lapland
(http://www.cbk.pan.wroc.pl/body/publikacje/2009/js_saariselka_sphinx.pdf)
- [79] Lin C H, Basu S and Li L 2009 *Solar Phys.* **257** 37 [arXiv:0809.1427v1 [astro-ph]]
- [80] Peres G, Orlando S, Reale F, Rosner R, Hudson H 2000 *ApJ.* **528** 537
- [81] Grotrian W 1939 *Naturwissenschaften* **27** 214
- [82] Shibata K, Nakamura T, Matsumoto T, Otsuji K, Okamoto T J, Nishizuka N, Kawate T, Watanabe H, Nagata S, UeNo S, Kitai R, Nozawa S, Tsuneta S, Suematsu Y, Ichimoto K, Shimizu T, Katsukawa Y, Tarbell T D, Berger T E, Lites B W, Shine R A and Title A M 2007 *Science* Vol. **318**, Issue 5856, pp. 1591, [arXiv:0810.3974v1 [astro-ph]]
- [83] <http://www.astro.umass.edu/~weinberg/a114/lectures/lec13.pdf>
- [84] Zioutas K, Dennerl K, Grande M, Hoffmann D H H, Huovelin J, Lakic B, Orlando S, Ortiz A, Papaevangelou Th, Semertzidis Y, Tzamarias Sp and Vilhu O 2006 *J. Phys. : Conf. Series* **39** 103 [astro-ph/0603507v1]
- [85] Hoffmann D H H and Zioutas K 2006 *Nucl. Phys. B Proc. Suppl.* **151** 359
- [86] Zioutas K, Tsagri M, Semertzidis Y, Papaevangelou Th, Nordt A and Anastassopoulos V 2007

- Proc. Int. Conf. on Identification of Dark Matter (Rhodes)* (World Scientific) p 372 [astro-ph/0701627v6]
- [87] <http://www.sciencedaily.com/releases/1997/11/971107071300.htm> and <http://www.sciencedaily.com/releases/2008/03/080306183137.htm>
- [88] Di Lella L and Zioutas K 2003 *Astropart. Phys.* **13** 145
- [89] Zioutas K, Dennerl K, Di Lella L, Hoffmann D H H , Jacoby J and Papaevangelou T 2004 *ApJ.* **607** 575-579
- [90] Zioutas K, Hoffmann D H H, Dennerl K and Papaevangelou T 2004 *Science* **306** 1485
- [91] Judge P 2008 *ApJ.* **683** L87-L90
- [92] <http://solar.bnsc.rl.ac.uk/newsletter/issue4/latest.shtml#coronalheating>
- [93] Klimchuk J A and Gary D E 1995 *ApJ.* **448** 925
- [94] Nindos A, Kundu M R, White S M, Shibasaki K and Gopalswamy N 2000 *ApJ. SUPPL* **130** 485
- [95] Ko Y K, Doschek G A, Warren H P and Young P R 2009 *ApJ.* **697** 1956 [arXiv:0903.3029v1 [astro-ph.SR]]
- [96] Reale F, Testa P, Klimchuk J A and Parenti S 2009 Evidence of widespread hot plasma in a non-flaring coronal active region from Hinode/XRT *Preprint* arXiv:0904.0878v1 [astro-ph.SR]
- [97] Schmelz J T, Saar S H, DeLuca E E, Golub L, Kashyap V L, Weber M A and Klimchuk J A 2009 *ApJ.* **693** L131-L135 [arXiv:0901.3122v1 [astro-ph.SR]]
- [98] Hannah I G , Hudson H S, Hurford G J, Lin R P 2008 *Constraining the Properties of Hard X-ray Nanoflares with RHESSI Observations of the Quiet Sun*, ed. H. Peter, Proc. 12th European Solar Phys. Meeting, 8-12 September 2008, Freiburg, Germany, (http://espm.kis.uni-freiburg.de/fileadmin/user_upload/espm/Proceedings-Talks/t.2.3-06.pdf)
- [99] Howard R 1974 *Solar Phys.* **38** 59
- [100] Christe S, Hannah I G, Krucker S, McTiernan J and Lin R P 2008 *ApJ.* **677** 1385
- [101] Centeno R, Socas-Navarro H, Lites B, Kubo M, Frank Z, Shine R, Tarbell T, Title A, Ichimoto K, Tsuneta S, Katsukawa Y, Suematsu Y, Shimizu T and Nagata S 2008 *ApJ.* **666** L137-L140
- [102] Guendelman E I 2008 *Phys. Lett. B* **662** 445-448
- [103] Guendelman E I 2009, private communication
- [104] Zioutas Z, Tsagri M, Semertzidis Y, Papaevangelou T, Nordt A and Anastassopoulos V 2008 *Proc. 4th Patras Workshop on axions, WIMPs, WISPs* DESY, Hamburg, Germany, 16-21 June 2008 (<http://axion-wimp.desy.de/e30>)
- [105] Ning Z 2008 *ApJ.* **686** 674-685
- [106] RHESSI Science Nuggets, <http://sprg.ssl.berkeley.edu/~tohban/nuggets/>
- [107] PDG 2006 *J. Phys. G: Nucl. Part. Phys.* **33** 265
- [108] Christensen-Dalsgaard J *et al* 1996 *Science* **272** 1286-1292
(see also http://bigcat.ifa.au.dk/~jcd/solar_models/)
- [109] Aschwanden M 2004 *Physics of the Solar Corona* (Springer) p 24-26 (http://books.google.ch/books?id=W7FE5_aowEQC)
- [110] Hudson H 2009, private communication
- [111] Zioutas K 2009 *CERN COURIER* **48(#5)** 19 (<http://cerncourier.com/cws/article/cern/34259>)
- [112] Cui Y, Li R, Zhang L, He Y and Wang H 2006 *Solar Physics* **237** 45
- [113] Cui Y, Li R, Wang H and He H 2007 *Solar Physics* **242** 1